# Chapter 18
# Negative Electrodes in Other Rechargeable Aqueous Systems

## 18.1 Introduction

This chapter discusses two examples of negative electrodes that are used in several aqueous electrolyte battery systems, the "cadmium" electrode and metal hydride electrodes.

It will be seen that these operate in quite different ways. In the first case, the "cadmium" electrode is actually a two-phase system, with elemental cadmium in equilibrium with another solid, its hydroxide. And in the second, hydrogen is exchanged between a solid metal hydride and hydrogen-containing ionic species in the electrolyte.

## 18.2 The "Cadmium" Electrode

### *18.2.1 Introduction*

Cadmium/nickel, Ni/Cd, or NiCad, cells have been important products for many years. They have alkaline electrolytes and use the "*nickel*" positive electrode, $H_xNiO_2$, which is discussed in the next chapter. Because they have both higher capacity and a reduced problem with environmental pollution—cadmium is considered to be environmentally hazardous—batteries with metal hydride, rather than cadmium, negative electrodes are gradually taking a larger part of the market. They are discussed later.



R.A. Huggins, *Energy Storage*, DOI 10.1007/978-3-319-21239-5_18

### 18.2.2 Thermodynamic Relationships in the H-Cd-O System

As in the case of the H-Zn-O system described in the last chapter, the first step in understanding what determines the potential of the cadmium electrode involves the use of available thermodynamic data to determine the relevant ternary phase stability diagram, for the driving forces of electrochemical reactions are the related reactions between electrically neutral species.

In this case, the key issue is the value of the Gibbs free energy of formation of CdO, which has been found to be −229.3 kJ/mol at 25 °C. This is less than the value for the formation of water, so a tie line between water and cadmium must be more stable than a tie line between CdO and hydrogen. Also, $Cd(OH)_2$ is a stable phase between water and CdO, because its Gibbs free energy of formation at 25°C is −473.8 kJ/mol, whereas the sum of the others is −466.4 kJ/mol. From these data the ternary phase stability diagram shown in Fig. 18.1 can be drawn. It is clear that it is different from the one for the H-Zn-O system discussed elsewhere.

It is seen that $Cd(OH)_2$ is also stable when Cd is in contact with water. The potential of the cadmium electrode is determined by the potential of the sub-triangle that has water, $Cd(OH)_2$, and cadmium at its corners.

Since there are three phases as well as three components, Cd, hydrogen, and oxygen, present, there are no degrees of freedom, according to the Gibbs phase rule, as discussed earlier. Therefore, the cadmium reaction should occur at a constant potential, independent of the state of charge. This is what is experimentally found.

The potential of all compositions in this triangle is determined by the reaction

$$^1/_2O_2 + Cd + H_2O = Cd(OH)_2 \tag{18.1}$$

and from the Gibbs free energies of formation of the relevant phases it is found that its value is −1.226 V relative to that of pure oxygen, as is shown in Fig. 17.2.

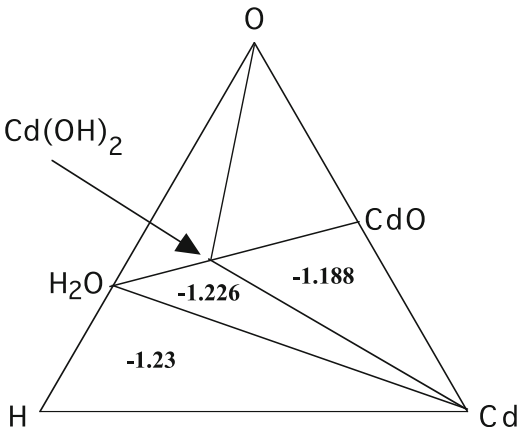


**Fig. 18.1** The H-Cd-O ternary phase stability diagram, showing the potentials of the compositions in the sub-triangles versus pure oxygen, in volts

The discharge of the cadmium electrode can be written as an electrochemical reaction:

$$Cd + 2(OH)^- = Cd(OH)_2 + 2e^- \tag{18.2}$$

This shows that there is consumption of water from the electrolyte during discharge, as can also be seen in the neutral species reaction in Eq. 18.1. This consumption of water must be considered in the determination of the electrolyte composition.

### *18.2.3 Comments on the Mechanism of Operation of the Cadmium Electrode*

There is another matter to be considered in the behavior of the cadmium electrode, since discharge involves the formation of a layer of $Cd(OH)_2$ on top of the Cd. This would require a mechanism to either transport $Cd^{2+}$ or $OH^{--}$ ions through the growing $Cd(OH)_2$ layer, both of which seem unlikely. This reaction is generally thought to involve the formation of an intermediate species that is soluble in the KOH electrolyte. The most likely intermediate species is evidently $Cd(OH)_3^-$.

The kinetics of the cadmium electrode are sufficiently rapid that the potential changes relatively little on either charge or discharge. Typical values are a deviation of 60 mV during charge, and 15 mV during discharge at the C/2, or 2-h, rate. In addition, there are small potential overshoots at the beginning in both directions if the full capacity had been employed in the previous step. This is, of course, what would be expected if the microstructure started with only one phase, and the second phase has to be nucleated. This is shown in Fig. 18.2 [1].

One of the questions that had arisen in earlier considerations of the mechanism of this electrode was the possibility of the formation of CdO. X-ray investigations have found no evidence for its presence. Thus if this phase were present it would have to be either as extremely thin layers or be amorphous.

However, this question can be readily answered by consideration of the potential of the reaction in the triangle with Cd, CdO and $Cd(OH)_2$ at its corners. This can be determined simply by the reaction along its edge:

$$^1\!/_2 O_2 + Cd = CdO \tag{18.3}$$

From the Gibbs free energy of formation of CdO this is found to be −1.188 V relative to the potential of oxygen. This is 38 mV positive of the equilibrium potential of the main reaction. Since it is not expected that the electrode potential would deviate so far during operation of these electrodes, the formation of CdO is unlikely.

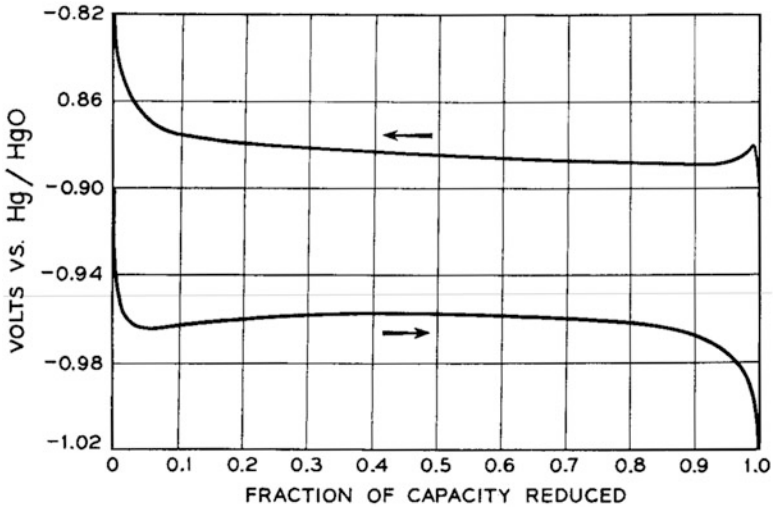


**Fig. 18.2** The charge–discharge behavior of a sintered-plate cadmium electrode, measured at about the C/2 rate in 2M KOH at 25 °C

## 18.3 Metal Hydride Electrodes

### *18.3.1 Introduction*

Metal hydrides are currently used as the negative electrode reactant in large numbers of reversible commercial batteries with aqueous electrolytes, generally in combination with "nickel" positive electrodes.

There are several families of metal hydrides, and the electrochemical properties of some of these materials are comparable to those of cadmium. Developmental efforts have led to the production of small consumer batteries with comparable kinetics, but with up to twice the energy content per unit volume of comparable small "normal" Cd/Ni cells. Typical values for AA size cells are shown in Table 18.1. For this reason, as well as because of the poisonous nature of cadmium, hydride cells are taking a larger and larger portion of this market.

### *18.3.2 Comments on the Development of Commercial Metal Hydride Electrode Batteries*

Although there had been research activities earlier in several laboratories, work on the commercialization of small metal hydride electrode cells began in Japan's Government Industry Research Institute laboratory in Osaka (GIRIO) in 1975. By

**Table 18.1** Typical capacities of AA size cells used in many small electronic devices

| Type of cell | $mWh/cm^3$ |
|---|---|
| "Normal" Cd/Ni | 110 |
| "High-capacity" Cd/Ni | 150 |
| Hydride/Ni | 200 |

1991 there were a number of major producers in Japan, and the annual production rate had reached about 1 million cells. Activities were also underway in other countries. Those early cells had specific capacity values of about 54 Wh/kg and specific powers of about 200 W/kg.

The production rate grew rapidly, reaching an annual rate of about 100 million in 1993, and over 1 billion cells in 2005. The properties of these small consumer cells also improved greatly. By 2006 the specific capacity had reached 100 Wh/kg, and the specific power 1200 W/kg. The energy density values also improved, so that they are now up to 420 Wh/l.

They are generally designed with excess negative electrode capacity, i.e., $N/P > 1$. This is increased for higher power applications.

The metal hydrides used in small consumer cells are multicomponent metallic alloys, typically containing about 30 % rare earths. Prior to this development, the largest commercial use of rare earth materials was for specialty magnets. The major source of these materials is in China, where they are inexpensive and very abundant. Rare earths are also available in large quantities in the USA and South Africa.

In addition to the large current production of small consumer batteries, development efforts have been aimed at the production of larger cells with capacities of 30–100 A h at 12 V. The primary force that is driving this move toward larger cells is their use in hybrid electric vehicles. In order to meet the high power requirements, the specific capacity if these cells has to be sacrificed somewhat, down to about 45–60 Wh/kg.

### *18.3.3 Hydride Materials Currently Being Used*

There are two major families of hydrides currently being produced that can be roughly described as $AB_5$ and $AB_2$ alloys.

The $AB_5$ alloys are based upon the pioneering work in the Philips laboratory that started with the serendipitous discovery of the reaction of gaseous hydrogen with $LaNi_5$. The basic crystal structure is of the layered hexagonal $CaCu_5$ type. Alternate layers contain both lanthanum and nickel, and only nickel. This structure is illustrated in Fig. 18.3.

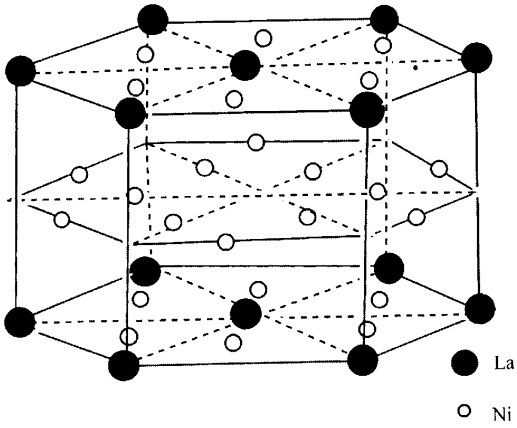


**Fig. 18.3** Schematic view of the layered hexagonal lattice of $LaNi_5$ [1]

The reaction of hydrogen with materials of this type can be written as

$$3H_2 + LaNi_5 = LaNi_5H_6 \tag{18.4}$$

The hydrogen atoms reside in tetrahedral interstitial sites between the host atoms. It has been found that hydrogen can occupy interstitial sites in suitable alloys in which the "*holes*" have spherical radii of at least 0.4 Å. In larger interstitial positions hydrogen atoms are often "*off center*."

Developmental work has involved the partial or complete replacement of the lanthanum with other metals, predominantly with Mischmetall (Mm), a mixture of rare earth elements, and zirconium. A typical composition of the relatively inexpensive Mischmetall is 45–58 % Ce, 20–27 % La, 13–20 % Nd, and 3–8 % Pr.

In addition, it has been found advantageous to replace some or all of the nickel with other elements, such as aluminum, manganese and cobalt. Furthermore, it is possible to change the A/B ratio. One major producer uses a composition that has a higher A/B ratio than 5, in the direction of $A_2B_7$, for example. These materials show relatively flat two-phase discharge voltage plateaus, indicating a reconstitution reaction. Various compositional factors influence the pressure (cell voltage) and the hydrogen (charge) capacity of the electrode, as well as the cycle life. There has also been a lot of developmental work on preparative methods and the influence of microstructure upon the kinetic and cycle life properties of small cells with these materials.

#### 18.3.3.1 Disproportionation and Activation

Another reaction between hydrogen and these alloys can also take place, particularly at elevated temperatures. It can be written as

$$H_2 + LaNi_5 = LaH_2 + 5Ni \tag{18.5}$$

and is called *disproportionation*. At 298 K the Gibbs free energies of formation of $LaNi_5$ and $LaH_2$ are −67 kJ/mol and −171 kJ/mol, respectively, so there is a significant driving force for this to occur, at least on the surface. Experiments have shown that the surface tends to contain regions that are rich in lanthanum, combined with oxygen. In addition, there are clusters of nickel. Because of the presence of these nickel islands, which are permeable to hydrogen, hydrogen can get into the interior of the alloy.

It is often found that a cyclic activation process is necessary in order to get full reaction of hydrogen with the total alloy. As hydrogen works its way into the interior there is a local volume expansion that often causes cracking and the formation of new fresh surfaces that are not covered with oxygen. This cracking can cause the bulk material to be converted into a powder, and is called *decrepitation*.

### *18.3.4 Pressure—Composition Relation*

If the particle size is small and there are no surface contamination or activation problems, the $LaNi_5$ alloy reacts readily with hydrogen at a few atmospheres pressure. This is illustrated in Fig. 18.4.

This flat curve is an indication that this is a reconstitution, rather than insertion, reaction.

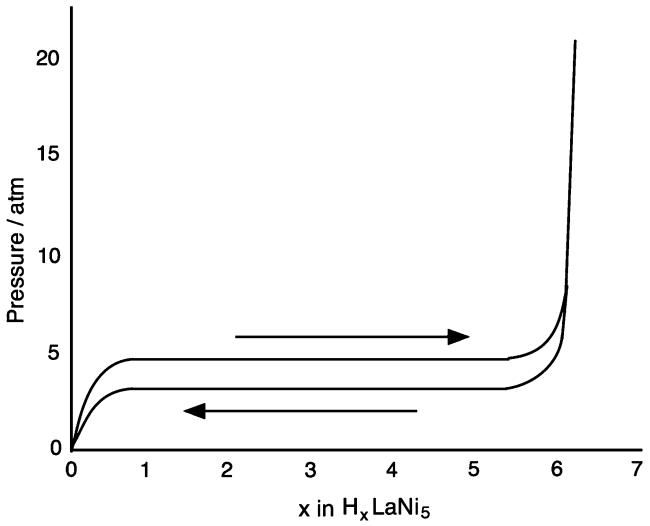


**Fig. 18.4** Schematic pressure–composition isotherm for the reaction of $LaNi_5$ with hydrogen

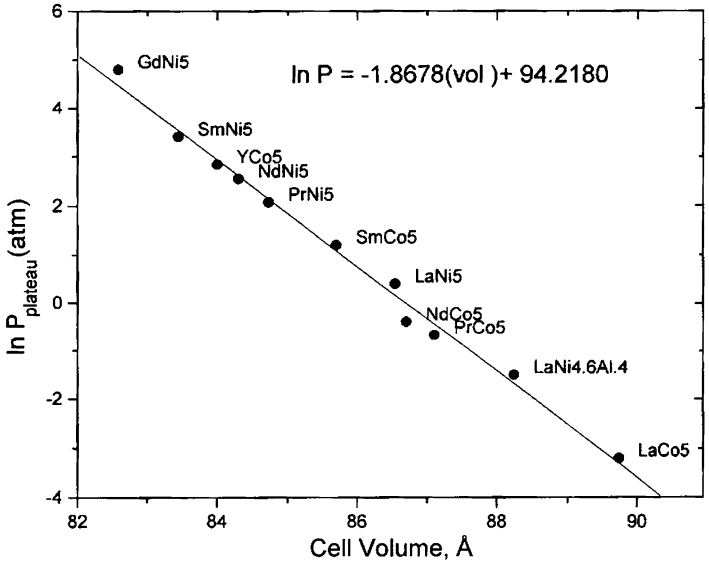


**Fig. 18.5** Relation between the logarithm of the plateau pressure and the volume of the crystal structure's unit cell. After [3]

There is a slight difference in the potential when hydrogen is added from that when hydrogen is removed. This hysteresis is probably related to the mechanical work that must occur due to the volume change in the reaction.

The pressure plateaus for the alloys that are used in batteries are a bit lower, so that the electrochemical potential remains somewhat positive of that for the evolution of hydrogen on the negative electrode.

It has been found that the logarithm of the potential at which this reaction occurs depends linearly upon the lattice parameter of the host material for this family of alloys. This is shown in Fig. 18.5.

In order to reduce the blocking of the surface by oxygen, as well as to help hold the particles together, thin layers of either copper or nickel are sometimes put on their surfaces by the use of electroless plating methods [3]. PVDF or a similar material is also often used as a binder.

### *18.3.5 The Influence of Temperature*

The equilibrium pressure over all metal hydride materials increases at higher temperatures. This is shown schematically in Fig. 18.6.

The relation between the potential plateau pressure and the temperature is generally expressed in terms of the Van't Hoff equation

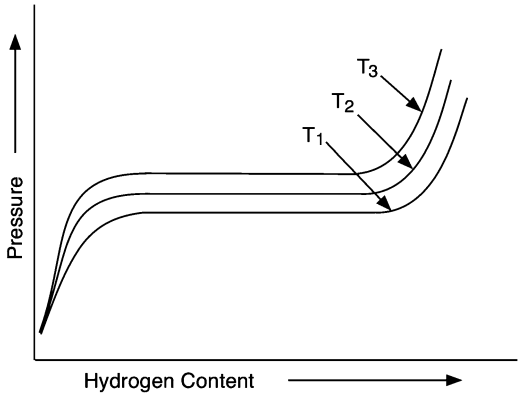


**Fig. 18.6** Schematic variation of the equilibrium pressure of a metal hydride system with temperature

$$\ln p(H_2) = \left({}^{\Delta H}/_{RT}\right) - \left({}^{\Delta S}/_{\mathrm{R}}\right) \tag{18.6}$$

This can readily be derived from the general relations

$$\Delta G = RT \ln p(H_2) \tag{18.7}$$

and

$$\Delta G = \Delta H - T\Delta S \tag{18.8}$$

This relationship is shown in Fig. 18.7 for $LaNi_5$ and a commercial Mischmetall-containing alloy [2]. It can be seen that the pressure is lower, and thus the electrical potential is higher, in the case of the practical alloy.

This type of representation is often use to compare metal hydride systems that are of interest for the storage of hydrogen from the gas phase. Figure 18.8 is an example of such a plot [3].

It can be seen that the range of temperature and pressure that can be considered for the storage of hydrogen gas is much greater than that which is of interest for the use in aqueous electrolyte battery systems.

Higher pressure in gas systems is equivalent to a lower potential in an electrochemical cell, as can be readily seen from the Nernst equation

$$E = -\left({}^{RT}/_{zF}\right) \ln p(H_2) \tag{18.9}$$

The reaction potential must be above that for the evolution of hydrogen, and if it is too high, the cell voltage is reduced. As a result, the range of materials is quite constrained, and a considerable amount of effort has been invested in making minor modifications by changes in the alloy composition.

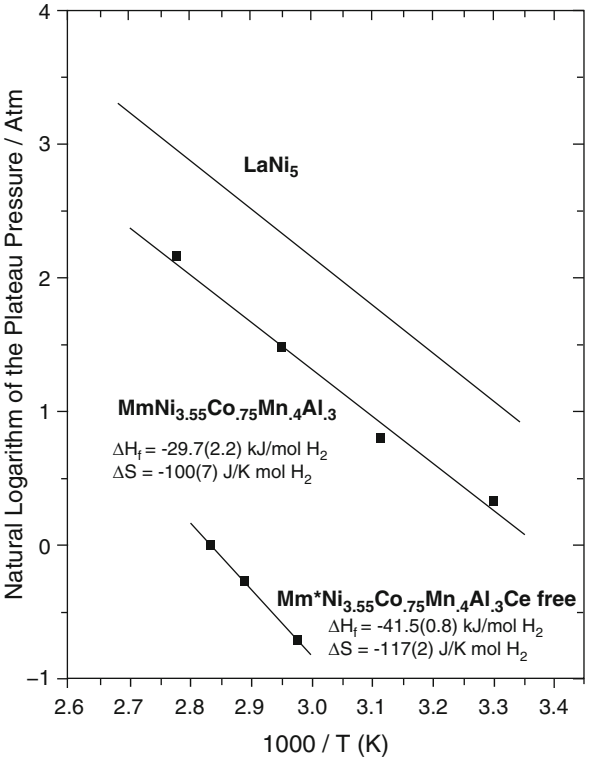


**Fig. 18.7** Van't Hoff plot for $LaNi_5H_x$ and two compositions of a $MmNi_{3.55}Co_{0.75}Mn_{0.4}Al_{0.3}H_x$ alloy. After [2]

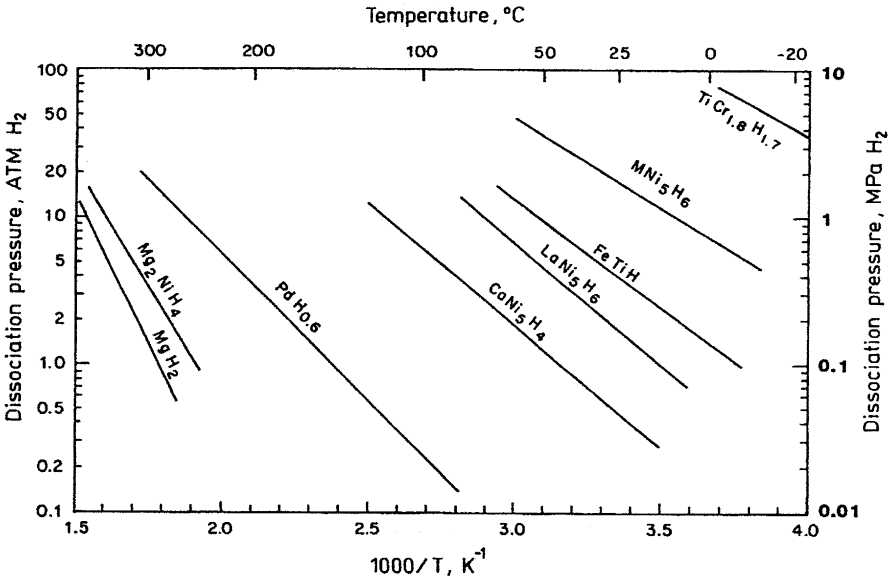


**Fig. 18.8** Example of Van't Hoff plot showing data for a wide range of materials. After [3]

### 18.3.6 $AB_2$ Alloys

The other major group of materials that are now being used as battery electrodes are the $AB_2$ alloys. There are two general types of $AB_2$ structures, sometimes called Friauf-Laves phases; the C14, or $MgZn_2$, type in which the B atoms are in a close packed hexagonal array, and the C15, or $MgCu_2$, type in which the B atoms are arranged in a close packed cubic array. Many materials can be prepared with these, or closely related, structures. The A atoms are generally either Ti or Zr. The B elements can be V, Ni, Cr, Mn, Fe, Co, Mo, Cu, and Zn. Some examples are listed in Table 18.2.

It has generally been found that the C14-type structure is more suitable for hydrogen storage applications. A typical composition can be written as (Ti,Zr) $(V,Ni,Cr)_2$.

### 18.3.7 General Comparison of These Two Structural Types

Both of these systems can provide a high charge storage density. Present data indicate that this can be slightly (5–10 %) higher for some of the $AB_2$ than the $AB_5$ materials.

However, there is a significant difference in the electrochemical characteristics of these two families of alloys. As illustrated in Fig. 18.4, the hydrogen pressure is essentially independent of the composition over a wide range in the $AB_5$ case. Thus the cell potential is independent of the state of charge, characteristic of a reconstitution reaction. On the other hand, the hydrogen activity generally varies appreciably with the state of charge in the $AB_2$ alloys, giving charge-dependent cell voltages. The fact that the cell voltage decreases substantially during discharge of cells with the $AB_2$ alloy hydrides can be considered to be a significant disadvantage for the use of these materials in batteries.

A serious issue, particularly in the $AB_2$ materials, is the question of oxidation, and subsequent corrosion, particularly of the B metals. This can lead to drastic reductions in the capacity and cycle life, as well as causing a time-dependent increase in gaseous hydrogen pressure in the cell. Because of this, special pre-etching treatments have been developed to reduce this problem. The vanadium content of the surface is evidently particularly important.

**Table 18.2** Structures of $AB_2$-phase materials

| Material | C14 structure (hexagonal) | C15 structure (cubic) |
|---|---|---|
| $TiMn_2$ | X | |
| $ZrMn_2$ | X | |
| $ZrV_2$ | | X |
| $TiCr_2$ | X | X |
| $ZrCr_2$ | X | X |
| $ZrMo_2$ | | X |

### 18.3.8 Other Alloys That Have Not Been Used in Commercial Batteries

An alloy of the $AB_2$ type based upon Ti and Mn, with some V, is currently being used for the storage of gaseous hydrogen, rather than in batteries. One commercial application is in fuel cell-propelled submarines manufactured in Germany. However, its hydrogen activity range is too high to be applicable to use in batteries.

A number of years ago there was a development program in the Battelle laboratory in Switzerland funded by Daimler Benz aimed at the use of titanium–nickel materials of the general compositions $A_2B$ ($Ti_2Ni$) and AB (TiNi) for use in automobile starter batteries. This early work showed that if electrodes have the right composition and microstructure and are properly prepared, they can perform quite well for many cycles. However, this development was never commercialized.

An interesting side issue is the fact that the TiNi phase, which is very stable in KOH, is one of the materials that is known to be ferroelastic, and to have mechanical memory characteristics. Its mechanical deformation takes place by the formation and translation of twin boundaries, rather than by dislocation motion. As a result, it is highly ductile, yet extremely resistant to fracture. Thus it would be interesting to consider the use of minor amounts of this phase as a metallic binder in hydride, or other, electrodes. It should be able to accommodate the repeated microscopic mechanical deformation that typically occurs within the electrode structure upon cycling without fracturing.

### 18.3.9 Microencapsulation of Hydride Particles

A method was developed some years ago in which a metallic coating of either copper or nickel is deposited by electro-less methods upon the hydride particles before the mechanical formation of the hydride electrode [4]. This ductile layer helps the formation of electrodes by pressing, acts as a binder, contributes to the electronic conductivity, and thus improves electrode kinetics, and helps against overcharge. It evidently also increases the cycle life. Since both copper and nickel do not corrode in KOH, this layer also acts to prevent oxidation and corrosion.

### 18.3.10 Other Binders

In addition to the copper or nickel metallic binders, some Japanese cells use PTFE, silicon rubber, or SEBS rubber as a binder. It has been found that this can greatly influence the utilization at high (up to 5C) rates. With the rubber binders (e.g. 3 wt% PTFE), flexible thin-sheet electrodes can be made that make fabrication of small spiral cells easier.

### 18.3.11 Inclusion of a Solid Electrolyte in the Negative Electrode of Hydride Cells

An interesting development was the work in Japan on the use of a proton-conducting solid electrolyte in the negative electrodes of hydride cells. This material is tetramethyl ammonium hydroxide pentahydrate, $(CH_3)_4NOH \cdot 5\ H_2O$, which has been called TMAH5. It is a clathrate hydrate, and melts (at about 70 °C) rather than decomposes, when it is heated. Thus it can be melted to impregnate a pre-formed porous electrode to act as an internal electrolyte. This is typically not true for other solid electrolytes, and can be advantageous in increasing the electrode–electrolyte contact area.

TMAH5 has a conductivity of about $5 \times 10^{-3}$ S/cm$^2$ at ambient temperatures. While this value is higher than the conductivity of almost all other known proton-conducting solid electrolytes, it is less than that of the normal KOH aqueous electrolyte. Thus if this solid electrolyte were to be used, one would have to be concerned with the development of fine-scale geometries. This could surely be done, but it would probably involve the use of screen printing or tape casting fabrication methods, rather than conventional electrode fabrication procedures.

Both hydride/$H_xNiO_2$ cells and hydride/$MnO_2$ cells have been produced using this solid electrolyte. Because of the lower potential of the $MnO_2$ positive electrode relative to the "nickel" electrode, the latter cells have lower voltages.

### 18.3.12 Maximum Theoretical Capacities of Various Metal Hydrides

The maximum theoretical specific capacities of various hydride negative electrode materials are listed in Table 18.3. Values are shown for both the hydrogen charged and uncharged weight bases. They include two $AB_5$ type alloys that are being used by major producers, as well as the basic $LaNi_5$ alloy and two $AB_2$ materials.

As would be expected, small commercial cells have practical values that are less than the theoretical maximum values presented in the last few pages. Hydride electrodes generally have specific capacities of 320–385 mAh/g. For comparison, the $H_xNiO_2$ "nickel" positive electrodes typically have practical capacities about 240 mAh/g.

**Table 18.3** Specific capacities of several $AB_5$ and $AB_2$ alloys

| Material | Uncharged, mAh/g | $H_2$ charged, mAh/g |
|---|---|---|
| $LaNi_5H_6$ | 371.90 | 366.81 |
| $MmNi_{3.5}Co_{0.7}Al_{0.8}H_6$ | 393.93 | 388.23 |
| $(LaNd)(NiCoSi)_5H_4$ | 248.80 | 246.51 |
| $TiMn_2$ | 509.67 | 500.16 |
| $(Ti,Zr)(V,Ni)_2$ | 448.78 | 441.39 |

## References

1. Milner PC, Thomas UB (1967) Adv Electrochem Electrochem Eng 5:1
2. Reilly JJ (1999) Handbook of Battery Materials. Besenhard JO (ed). Wiley-VCH, p. 209
3. Sandrock GD, Huston EL (1981) Chemtech 11:754
4. Sakai T, Yoshinaga H, Miyamura H, Kuriyama N, Ishikawa H (1992) J Alloys Compounds 180:37